Plasma Medicine 4(1-4): 177-191 (2014)

Spatially Resolved Optical Emission Spectroscopy of a Helium Plasma Jet and its Effects on Wound Healing Rate in a Diabetic Murine Model

Marc C. Jacofsky,[a] Cheri Lubahn,[b] Courtney McDonnell, [a]Yohan Seepersad,[c] Gregory Fridman,[c] Alexander Fridman,[c] & Danil Dobrynin[c]

[a]Cold Plasma Medical Technologies, Inc., Scottsdale, AZ, USA; [b]Sun Health Research Institute, Sun City, AZ, USA; [c]A.J. Drexel Plasma Institute, Drexel University, Philadelphia, PA, USA,

***Address all correspondence to:** Corresponding Author: Marc C Jacofsky, PhD, 8502 E. Princess Dr., Suite 210, Scottsdale AZ, 85255; Email: marc.jacofsky@plasmology4.com; T: 1.480.342.9840

ABSTRACT: A spatially resolved characterization of the active species generated in a pure helium plasma plume was performed using optical emission spectroscopy techniques. A qualitative assessment of the radiative species was conducted under various experimental conditions to determine the ideal flow rate and distance along the plume for maximal species production. Nitrogen radicals dominated the emission in the spectra, though measurable amounts of oxygen and OH were also observed, with a minimal radiative contribution from the He carrier gas. Radiative species were maximized 25–30 mm distal to the outflow orifice of the plasma generator.

A diabetic mouse model was then utilized to examine the effects of this pure helium plasma on the healing rates of large-area, full-thickness skin wounds. A total of 80 mice were included and were subjected to one of several treatment regimens: 30 seconds twice daily, 60 seconds twice daily, 90 seconds once daily, and helium gas control. Digital photographs were taken daily, and wound surface areas were quantified using image analysis software. Curves were then fit to daily wound surface areas to determine healing rates. Wounds healed significantly faster following plasma treatment. The maximum effect was obtained with 60-second treatments applied twice daily.

KEY WORDS: cold plasma, mouse, diabetes mellitus

I. INTRODUCTION

Plasma medicine is an emerging and rapidly maturing field that involves the application of nonthermal plasmas to biological tissues with the goal of treating a disease or disorder. The application of different types of cold plasma have been shown to improve wound healing, to reduce wound bacterial loads, to achieve rapid coagulation of bleeding, and even to reduce the size of malignant tumors. Lloyd et al. reviewed the use of gas jet plasmas for the treatment of wounds and infections, highlighting the great potential of this new technology platform.[1] More recent randomized clinical trials in humans have confirmed that cold plasmas demonstrate efficacy in the healing process of both acute and chronic wounds.[2–3]

The healing of chronic wounds can present a significant challenge to the patient and treating healthcare team. It has been well documented that patients with diabetes mellitus

1947-5764/14/$35.00

demonstrate slower rates of healing and are at increased risk for developing chronic wounds.[4] It has been reported that 15–25% of diabetic adults develop chronic diabetic wounds and that 14% of these patients will require some form of amputation.[4] With 7% of the US population (21 million people) affected by type II diabetes, the annual cost of treating diabetic wounds was approaching $10 billion dollars by 2007.[5] Standard therapeutic treatment techniques for these incalcitrant wounds include vacuum-assisted closure (VAC) therapies, frequent wet-dry dressing exchanges, and hyperbaric chamber treatments. These treatment options are all labor intensive, expensive, and inconvenient, and they usually require home health assistance or frequent trips to a wound care center. As the incidences of obesity and diabetes continue to increase in the United States and abroad, the frequency of these wounds is also increasing.[6] Therefore, new treatment modalities that provide improved outcomes and cost containment are desperately needed. The application of room-temperature plasma directly to the wound bed has shown promise in stimulating wound healing.

Due to differences in the wound closure mechanism between humans and mice, the use of murine models of wound healing in a manner predictive of human wound healing has been challenging.[11–16] Mice generally heal by contraction of the wound margins, whereas humans heal primarily through reepithelialization and granular tissue formation.[12] The use of occlusive coverings placed on the wound bed limit the degree of contraction around the wound margins, which can reduce contraction and lead to a more "human-like" pattern of wound healing.[13,14] With these techniques, unchallenged wounds (those without bacterial load) generally heal to full closure in 10–14 days whereas challenged wounds (i.e., severely infected) can take up to 21 days to heal completely. Without these techniques, mouse wounds simply heal too quickly and completely to study the effects of different wound treatment modalities.

Prior to testing, a spatially resolved characterization of the active species generated in the plume of the jet was performed via optical emission spectroscopy techniques. A qualitative assessment of the radiative species was done under various experimental conditions. The effects of changing the substrate at the exit of the plume, the addition of small amounts of oxygen, and species generation as a function of changing flow rate were studied. Quantification of plasma properties based on analysis of the spectra was not done because it was irrelevant to the scope of the work presented here. The characterization was performed as a means of determining the appropriate conditions to achieve maximum plasma energy levels for wound delivery, represented by the active species in the plume. This information is important to determining the appropriate device parameters such as, flow rate, distance of jet from treatment area and gas composition.

II. MATERIALS AND METHODS

A. Active Species Characterization of the Helium Jet

The principle of operation of the atmospheric pressure plasma jet used in these experiments is highlighted in the schematic shown in Fig. 1. The flow rate of the gas mixture

into the reactor is controlled by mass flow controllers connected in line with the feed gas supplies (Alicat Scientific, MC-0.5SCCM-D). In these experiments, gas flow rates were chosen such that the emitted plume from the jet maintained a fully developed structure. When the flow rate was too low, the treatment surface needed to be very close to the jet nozzle, and the plume was not fully developed (Fig. 2). For the initial experiments, the jet nozzle was kept at a constant distance of 35 mm above the grounded treatment surface below it. Below a flow rate of 9.44 liters per minute (LPM), the stable and fully developed jet plume could not be formed at a nozzle–surface separation distance of 35 mm, and the radiative emission signal from the jet exhaust had a very low signal-to-noise ratio.

Optical emission spectroscopy was facilitated via a fiberoptic bundle (Princeton Instruments-Acton, 10 fibers, 200 μm core) connected to the spectrometer (Princeton Instruments, Acton Research, TriVista TR555 spectrometer system with PIMAX digital ICCD camera, Trenton, NJ). Light is collected from various positions along the length of the plume, the positions of which are distinguished in the results. The slit entrance for the spectrometer setup was 200 μm, and instrument broadening was <1 nm. These parameters were not an issue as the data were collected as a means to qualitatively analyze the differences in species concentrations along the jet plume, and not for quantification of absolute values or calculation of plasma parameters. Results have not been corrected for the wavelength response variation of the detector.

B. Medical Testing

A helium plasma jet was applied to full-thickness wounds created on the backs of 80 mice genetically predisposed to early development of type II diabetes (BKS.Cg–+Lepr^{db} +Lep-

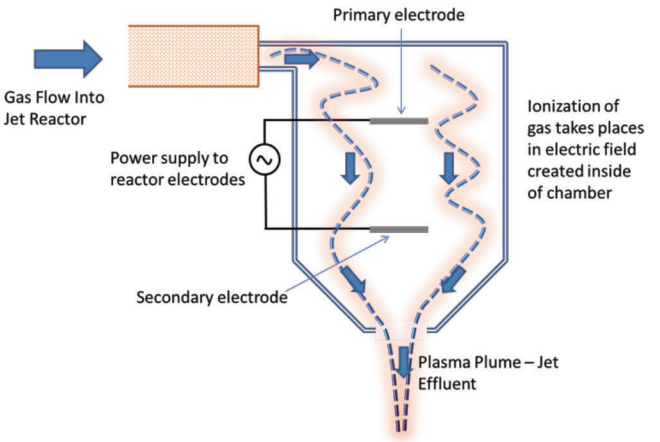

FIG. 1: Simplified schematic of atmospheric pressure plasma jet used in the experiments

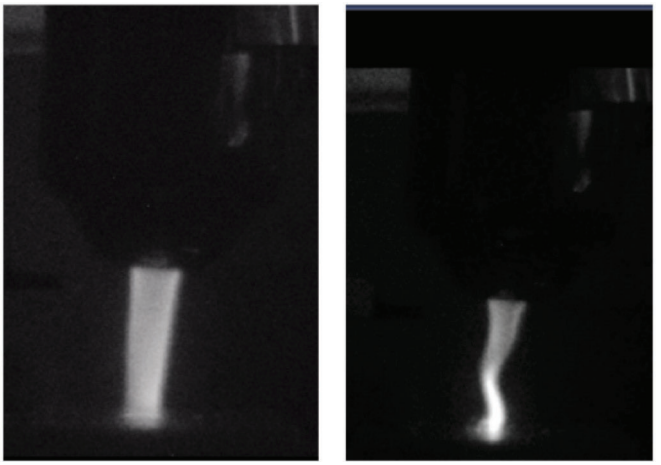

FIG. 2: Stable jet plume (left) and unstable jet plume (right). Jet plume stability was dependent on flow rate

r^{db} OlaHsd, Harlan Laboratories). All mice were females 10 weeks of age and already exhibited marked obesity. The hair was sheared from the dorsal aspect of each animal, and the skin was cleansed with providone-iodine solution followed by isopropyl alcohol. Following anaesthetization with isoflurane inhalation, a template was placed on the skin, and an area measuring 15 mm rostrocaudally by 10 mm mediolaterally was marked with a surgical marker. Surgical scissors were used to create full-thickness wounds with clean reproducible margins (Fig. 4). Animals were randomized to receive one of four treatment modalities and two survival durations (Table 1). The four treatment groups were established as follows: plasma 30 seconds twice daily (b.i.d.), plasma 60 seconds b.i.d., plasma 90 seconds once daily (qd), and controls, which received sham helium treatment 60 second b.i.d. from the same applicator and helium supply without power delivery.

The initial treatments were performed immediately after wounding and resumed the following morning on the schedule designated by grouping. All wounds were immediately covered with Tegaderm (3M, St Paul, MN) transparent semipermeable postoperative dressings (2.5 × 3.0 cm) prior to the animal being returned to its enclosure. The mice were treated for pain with a single dose of buprenorphine and demonstrated limited guarding, requiring no further analgesic. Following recovery from anesthesia, all animals were returned to their enclosures and were permitted free access to food and water. Tegaderm dressings were replaced with fresh coverings after each treatment session. All components and procedures were approved prior to execution of the experiments by the Sun Health Research Institute's animal use and care committee and complied with all USDA and NIH guidelines for the care and use of laboratory animals.

The plasma applicator was positioned 20 mm from the surface of the wound bed in a static location using a laboratory ring stand. Mice were not anesthetized for each plas-

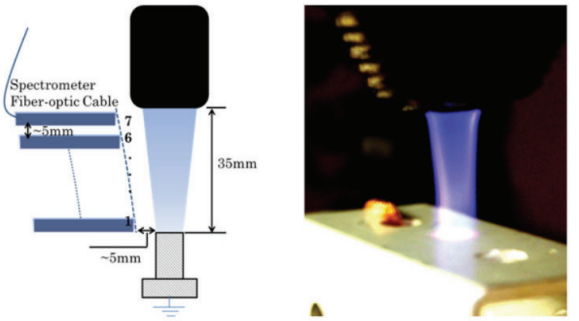

FIG. 3: Left: Schematic of the positioning of the optical fiber bundle for emission spectroscopy measurements. The numbers represent probe positions along the length of the plume. Right: Photograph of the jet plume impinging a metal base at a distance 3.5 cm from the nozzle exit

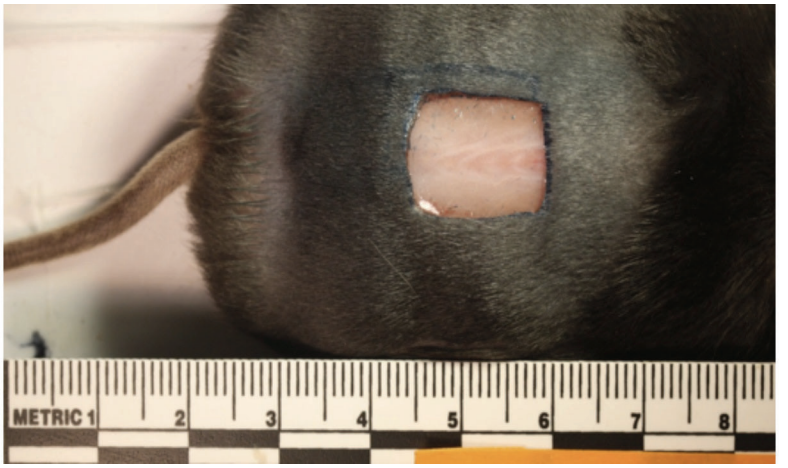

FIG. 4: Fresh full thickness wound on dorsal surface of mouse

ma/sham treatment so their response and behavior could be observed. They were placed into a restraint tube that restricted their movement but allowed access to their wounds Fig. 5. Pure UHP helium (>99.999% pure) was delivered at a flow rate of 16.5 LPM using a regulator. The electrode was energized with 25 KV peak radiofrequency energy at a pulse rate of 400 Hz, with each pulse lasting 40 μs.

All mice and respective wounds were photographed at the same time each day, immediately prior to receiving treatment. A scientific graded scale was placed in each photo in the same plane as the wound. Images were imported into ImageJ image analysis

software (National Institutes of Health) and were size corrected using the scale function. A blinded observer then placed control points along the margin of the wound using the polygon tool, and the surface area bounded by the polygon was recorded. The wound surface area for each animal, each day, was plotted, and a curve was fit to each animal's data set. The slope of this line indicates the wound healing rate, or the number of new square millimeters of new tissue formed each day. The slopes of each healing curve were then compared statistically using ANOVA. Post hoc testing for significant ANOVA was performed using two-tailed t-test for equal variance between all potential data pairs.

III. RESULTS

The results are divided into two distinct sections: the first presents the results from optical emission spectroscopy of the jet plume; the second presents the medical results from testing.

TABLE 1: Treatment groups and sacrifice schedule

Group/Treatment	Total Group Size	Sacrifice at day 5	Sacrifice at day 15
Control Diabetic Wound	20	10	10
Treated 30sec, b.i.d.	20	10	10
Treated 60sec, b.i.d.	20	10	10
Treated 90sec, qd	20	10	10
Total N	80	40	40

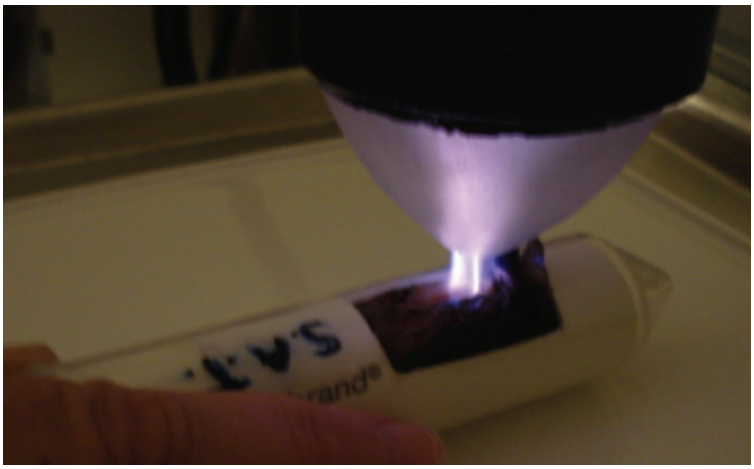

FIG. 5: Mouse in restraint tube being administered cold plasma treatment

A. Chemical Species Characterization

1. Spatial Characterization of Radiative Species

Emission spectra from the jet plume were collected from seven different points along the length of the plume, for a wavelength range of 250–1000 nm. This wavelength range contains electronic, vibrational, and rotational modes for various species including nitrogen, oxygen, and hydroxyl radicals. Uncalibrated measurement of the intensity of these transitions was used to infer the variation in concentrations of these radicals for various positions along the jet. The camera gate in these experiments was 2 seconds, and the gas flow rate was 11.8 LPM of pure helium. Care was taken to position the optical probe ~5 mm away from the jet plume at each position along its length (Fig. 3).

Figure 6 shows nitrogen species emission as it evolves roughly along the jet plume. The results show that maximum nitrogen excitation takes place farthest away from the jet nozzle, which can easily be explained by the increase in mixing with the ambient room air as the plume propagates. Close to the jet nozzle, where mostly the carrier gas (Helium) is exiting, there is little excitation of nitrogen species and, hence, the lowest emission intensity. The trends in emission intensity and concentration of various active species produced are shown in Fig. 7. The same explanation of gas mixing applies to the interpretation of these results. The results show that, at ~20 mm from the jet nozzle, the concentrations of most of the active species in the plasma are the greatest.

The flow rate of the gas through the jet was varied to investigate the effect of exit stream velocity on the production of active species. The gas volumetric flow rate was varied through 11.8, 16.5, and 23.6 LPM (25, 35, and 50 CFH), and the evolution of

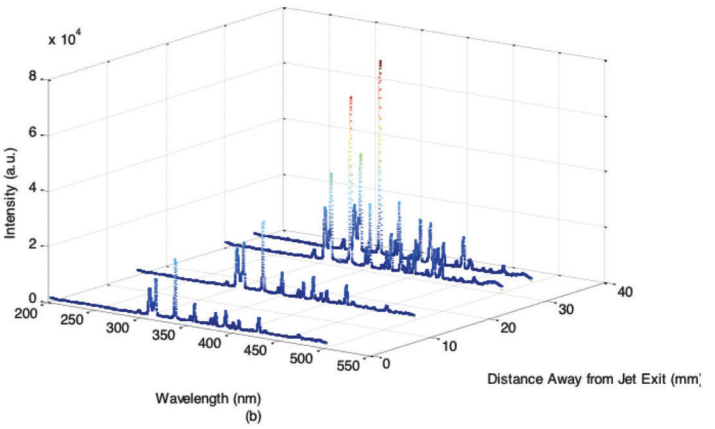

FIG. 6: Emission spectrum in the 300–420-nm wavelength range for the top (exit of nozzle), bottom (near end of jet plume), center of the jet plume, and at the contact of the substrate, for pure helium gas flow jet. The bottom figure shows the spatial dependence in expanded waterfall view

different species along the plume of the jet was measured. All other experimental conditions from the first experiment were maintained.

The results showing the intensity variation of the hydroxyl (OH) vibrational peak near 308 nm is shown in Fig. 8. Similar results for different species were recorded, and the data were consolidated into the results shown in Figs. 9−11. Consistent with the previous findings, the maximum active species production occurred near the lower end of the jet plume, measured here approximately 20 mm beyond the nozzle exit. The results also indicated that the optimal flow rate for generating active species did not occur when flow rate was the highest but rather at the moderate flow rate of 16.5 LPM.

2. Changes in Species Concentration and Development for Organic Versus Inorganic Substrate

The previous experiments were performed with the jet forming on a metal surface at the exit of the nozzle. The impact on active species generation as this substrate was changed to an organic surface was then investigated. An agarose gel was used to simulate organic tissue and held at a distance of 30 mm from the exit of the jet plume throughout different flow rates; the comparative pictures of the jet in both situations are shown in Fig. 12. The emission spectrum was again collected and analyzed to investigate the species concentrations along the plume of the jet. The results reveal identical trends in active species concentrations, with peak emission intensity occurring for moderate gas flow rates close to 20 mm away from the jet exit. It should be noted that a ground wire was placed in contact with the agar on the plate (Fig. 12). The relative intensity of active species generation was also roughly the same, with no significant change in concentrations of species generated over the two media.

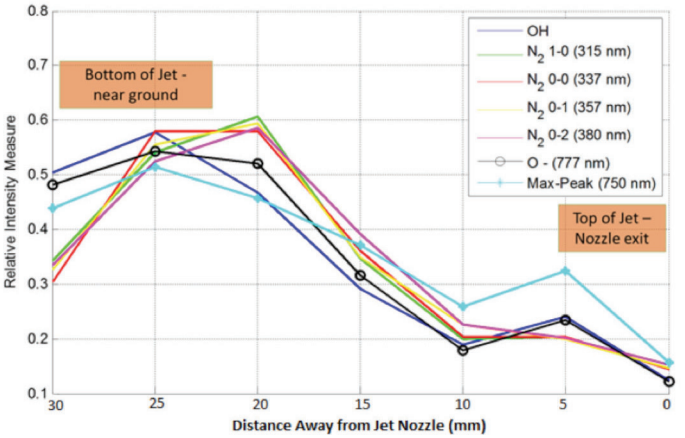

FIG. 7: Variation of the peak intensity for various emitting species across the plume of the jet. The position of the top of the jet and the bottom are indicated on the figure. The flow rate for these results was 11.8 LPM

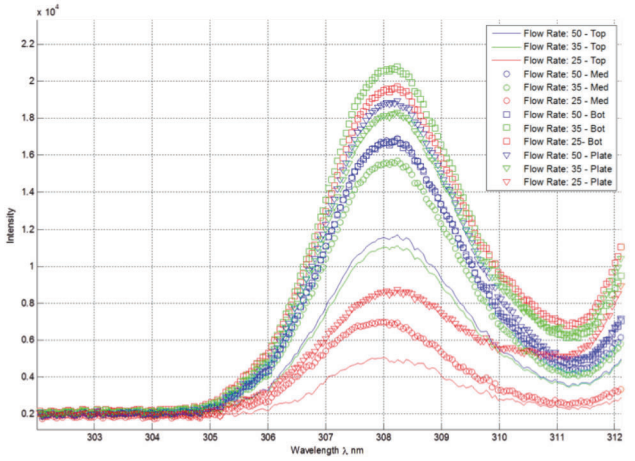

FIG. 8: OH band intensity for various flow rates and positions along the jet plume. The distinctions are as follows: Top, near the jet nozzle; Med, center of jet plume; Bot, near the bottom of the jet plume (5 mm above surface); Plate, emission from area of contact on plate; Positions (7), (5), (2), and (1) respectively according to Fig. 3

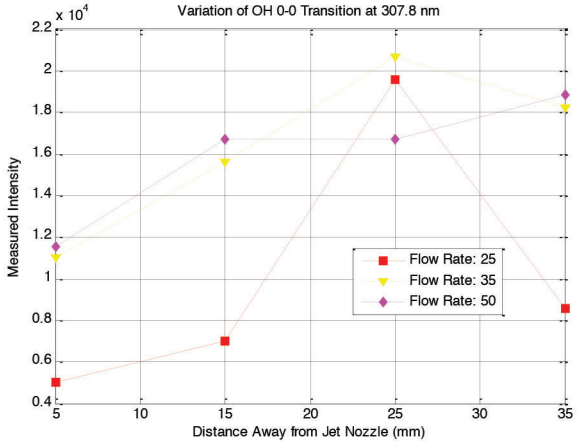

FIG. 9: Variation in emission intensity of OH 0–0 peak across the jet plume

B. Medical Testing

All animals tolerated the plasma and sham treatments well. No apparent signs of distress or adverse reactions were noted. All groups showed reductions in wound area over the 5-day treatment period. The helium-treated control animals showed an 8.7 mm^2/day

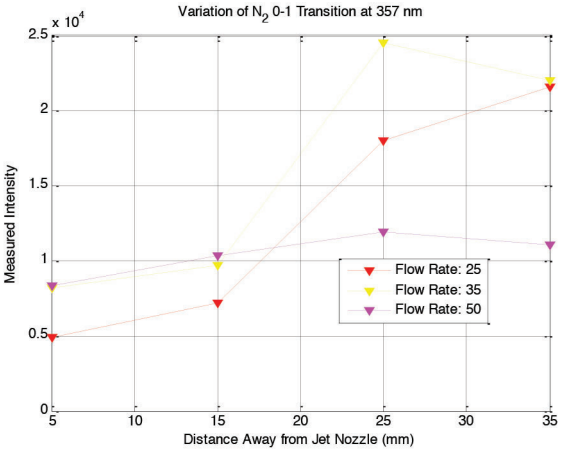

FIG. 10: Variation in emission intensity of N¬2 0–0 peak at 357 nm across the jet plume

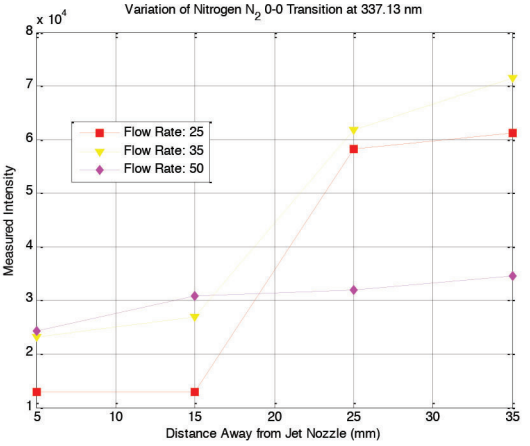

FIG. 11: Variation in emission intensity of N2 0–0 peak at 337.13 nm across the jet plume

reduction in wound size. In contrast, the animals treated with plasma in the 5-day survival group showed a marked increase in the rate of wound closure (Figs. 13 and 14). Figure 13 shows a linear curve fit to the wound size data for each treatment group as a whole. Therefore, the slope of the line indicates the aggregate rate of wound closure in square millimeters per day (mm^2/day) for each group. This plot demonstrates that the 60-second b.i.d. group exhibited the most rapid wound closure rate, 15.8 mm^2/day of surface area decrease, which was nearly double the wound closure rate of the control group. The 30-second b.i.d. group and the 90-second qd group had healing rates that were faster than controls but slower than the 60-second b.i.d. group. To calculate sta-

tistics between groups for these rates of closure, a linear fit was performed for the data for each individual animal over the 5-day healing period. Figure 14 shows the mean and standard deviations for each treatment group. A significant ANOVA *P* value of .011 was obtained when the wound closure rates between groups were compared. Post hoc testing indicates that statistical significance occurred between the 60-second b.i.d. group and all other treatment groups. The 30-second b.i.d. group and the 90-second qd group did not differ significantly from each other or the controls, although a trend for more rapid healing was detected. Notably, while the 90-second qd group's wounds did not close significantly more quickly than those of the control group or the 30-second b.i.d. group, they did subjectively appear to granulate more quickly.

For the 15-day-survival animals, the slopes of the healing curves were very similar and did not differ to the same extent as those observed in the 5-day-survival animals (Figs. 15 and 16). The ANOVA *P* value indicates no significant differences in the healing rates between groups (*P* =. 66).

IV. DISCUSSION

The results of optical emission spectroscopy of the jet plume are in good agreement with other findings from the literature.[17] The production of active species from nitrogen and oxygen increases farther away from the nozzle as entrainment with the surrounding air and the plasma gas from the jet takes place. For a constant distance between the jet nozzle and the grounded substrate, the flow rate is also important because it governs the turbulence in the jet plume. When the flow rate is too low, the jet plume cannot sustain the plasma to the substrate; when the flow rate is too high, mixing with the surrounding air is inhibited. No significant change in active species generation was expected from

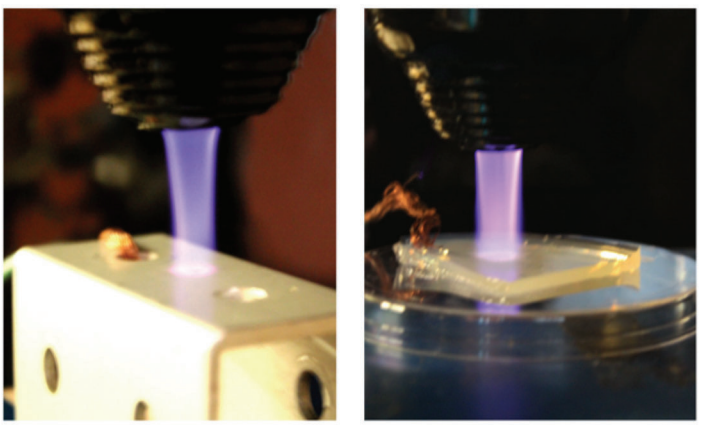

FIG. 12: Photograph showing formation of jet over metallic surface (left) and organic surface–agar (right)

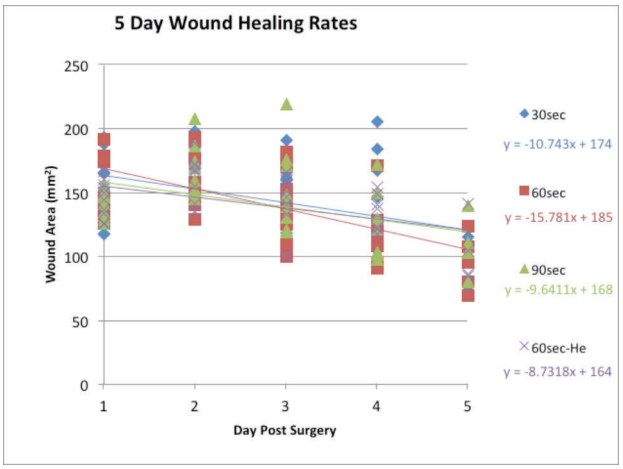

FIG. 13: Wound healing rates determined by linear curve fit to each group of 5-day-survival animals in aggregate

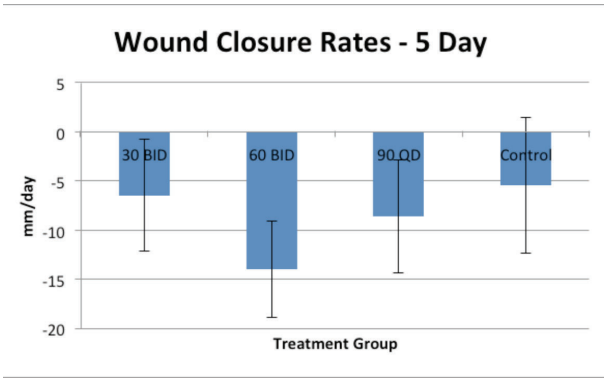

FIG. 14: Mean and standard deviation error bars for groups as calculated from individual 5-day-survival animals

the change in the substrate because secondary electron emission plays a small role in the chemistry induced in the jet plume, except close to the surface of the substrate.

The results of the 5-day healing rates in a diabetic mouse model indicate that cold plasma therapy dramatically increases the rate of wound closure. Specifically, treatments of 60 seconds twice daily showed the most dramatic improvement in wound healing, followed by treatments of 90 seconds once daily. This finding demonstrates that the "dosing" of plasma plays an important role in the observed biological effects. However, by 15 days of continued treatment, these benefits appeared to wane and healing rates between groups equalized. This finding suggests that plasma treatment may be most

beneficial during the first several days of wound healing, becoming less effective with continued use.

It was noted in the introduction that humans tend to heal through granulation processes and that animal models, specifically rodents, heal primarily through contraction. The techniques employed in this study to measure wound healing rates are far more sensitive to contraction than to granulation because the margins of the wound were recorded daily. Because an increase in granulation tissue was observed with longer-duration plasma treatments, albeit subjectively, it appears that the increased granulation may act to limit contraction of the wound. The granulation tissue that forms in the basal tissue layers of the wound act to splint the wound open and limit further rapid contraction. Therefore, the analysis performed may not be sensitive enough to detect improved healing through granulation or to detect a change in healing mechanism from one of primarily contraction to one of granulation. Analysis is ongoing to quantify this increase in granulation tissue from histological sections, but measuring thickness of tissue remain challenging on histology sections because preparation techniques introduce significant distortion during mounting and cutting.

If plasma treatment is only effective at improving wound healing over a limited duration in an acute wound, this finding would raise questions about the efficacy of cold plasma therapies in chronic wounds. Given that human clinical trials demonstrate improved healing in both acute and chronic wounds; this concern appears to be mitigated in practical use. Clinically speaking, chronic wounds are often debrided prior to interventions, which temporarily converts them to acute wounds and may open a window of opportunity for cold plasma therapies. This study used frequent, repetitive treatment modalities of generally short duration to establish some baseline values for future optimization. An exploration of a wider range of treatment modalities is warranted to optimize the effects

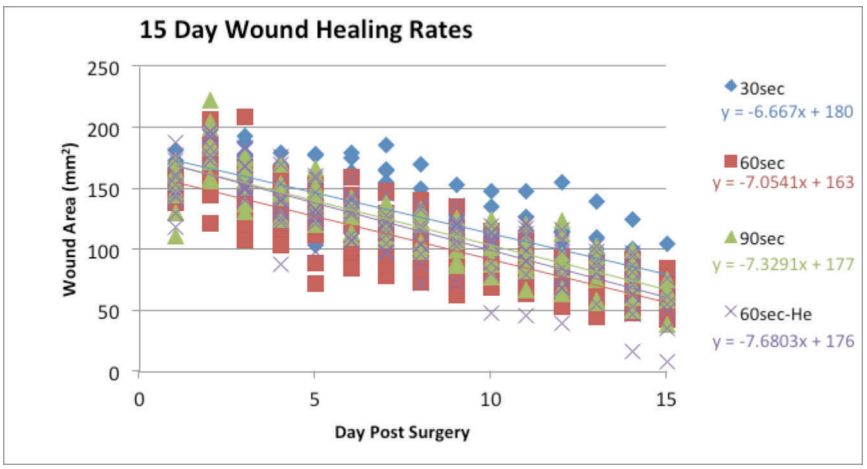

FIG. 15: Wound healing rates determined by linear curve fit to each group of 15-day-survival animals in aggregate

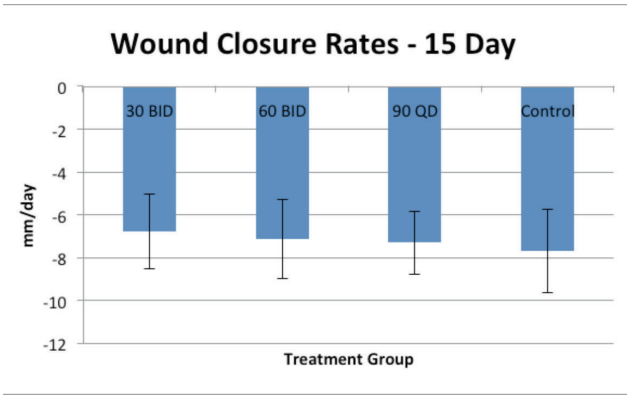

FIG. 16: Mean and standard deviation error bars for groups as calculated from individual 15-day-survival animals

of plasma treatment on these wounds. Specifically, treatments of 1 minute and longer at less frequent intervals deserve further exploration and would be more consistent with the practical clinical use of a plasma medicine system. Recovery time of cells between treatments may be critical to successful longer-term wound healing, as the cells are permitted to recover from the stress of the plasma treatment prior to the next treatment.

V. CONCLUSIONS

The cold plasma therapy employed in this study dramatically improved the healing rates of acute wounds in genetically diabetic mice through 5 days. These mice are slower to heal than their wild-type counterparts and exhibit parallels with diabetic human wound healing. If these results can be duplicated in humans suffering from diabetic wounds, improved clinical outcomes could be realized, leading to reductions in comorbidities such as amputation and related costs of care.

Production of chemically active species throughout the jet plume was shown to be tunable over the parameters of flow rate and distance from the substrate. In this regard, the parameters of the jet can be adjusted to appropriately control desired populations of active species. Maximum generation of all active species occurred around the 2-cm distance from the jet nozzle for an 11.8 LPM flow rate, though this position varies with flow rate. Nitrogen radicals dominated the emission in the spectra recorded, though measurable amounts of oxygen and OH were also observed, with a minimal radiative contribution from the He carrier gas. In future studies, a more quantitative approach of radiative species can be achieved through relatively simple calibration of the optical setup, which was not done in this work, or through the method described by Lu and Wu.[18] Further investigation is required to identify the mechanism linking wound healing capabilities to the plasma jet; that is, whether the radiation, chemical species, or electric

field plays a major role, or whether precise contributions of each factor yield optimal healing enhancement.

REFERENCES

1. Lloyd G, Fridman G, Jafri S, Schultz G, Fridman A, Harding K. Gas plasma: medical uses and developments in wound care. Plasma Process Polym. 2010;7:194–211.
2. Heinlin J, Zimmermann JL, Zeman F, Bunk W, Isbary G, Landthaler M, Maisch T, Monetti R, Morfill GE, Shimizu T, Steinbauer J, Stolz W, Karrer S. Randomized placebo-controlled pilot study using cold atmospheric argon plasma on skin graft donor sites. Wound Rep Reg. 2013;21(6):800–07.
3. Isbary G, Heinlin J, Shimizu T, Zimmermann JL, Morfill G, Schmidt H-U, Monetti R, Steffes B, Bunk W, Li Y, Klaempfl T, Karrer S, Landthaler M, Stolz W. Successful and safe use of 2 min cold atmospheric argon plasma in chronic wounds: results of a randomized controlled trial. Brit J Derm. 2012;167:404–10.
4. Trousdale RK, Jacobs S, Simhaee DA, Wu JK, Lustbader J. Wound closure and metabolic parameter variability in a db/db mouse model for diabetic ulcers. J Surg Res. 2009;151:100–07.
5. Michaels J, Churgin SS, Blechman KM, Greives MR, Aarabi S, Galiano RD, Gurtner GC. db/db mice exhibit severe wound-healing impairments compared with other murine diabetic strains in a silicone-splinted excisional wound model. Wound Rep Reg. 2007;15:665–70.
6. Scherer SS, Pietramaggiori G, Mathews JC, Orgill DP. Short periodic applications of the vacuum-assisted closure device causes an extended tissue response in the diabetic mouse. Plast Reconstr Surg. 2009;124:1458–65.
7. Croft CB and Tarin D. Ultrastructural studies of wound healing in mouse skin: I. Epithelial behaviour. J Anat. 1970;105(1): 63–7.
8. Leiter EH and Lee C. Mouse models and the genetics of diabetes. Is there evidence for genetic overlap between type 1 and type 2 diabetes?. Diabetes. 2005;54(Suppl 2):s151–s158.
9. Tkalcevic VI, Cuzic S, Parnham MJ, Pasalic I, Brajsa K. Differential evaluation of excisional non-occluded wound healing in db/db mice. Toxicol Path. 2009;37:183–92.
10. Pietramaggiori G, Scherer SS, Mathews JC, Alperovich M, Yang H, Neuwalder J, Czeczuga JM, Chan RK, Wagner CT, Orgill DP. Healing modulation induced by freeze-dried platelet-rich plasma and micronized allogenic dermis in a diabetic wound model. Wound Rep Reg. 2008;16(2):218–25.
11. Stepinska M, Grzybowski J, Struzyna J, Olszowska M, Jablonska H, Chomicka M, Chomiczewski K. Mouse model of infected wound. Acta Microbiol Pol. 1995;44(1):39–46.
12. Galiano RD, Michaels J, Dobryansky M, Levine JP, Gurtner GC. Quantitative and reproducible murine model of excisional wound healing. Wound Rep Reg. 2004;12:485–92.
13. Holder IA, Brown RL, Greenhalgh DG. Mouse models to study wound closure and topical treatment of infected wounds in healing-impared and normal healing hosts. Wound Rep Reg. 1997;5:198–204.
14. Simonetti O, Cirioni O, Goteri G, Ghiselli R, Kamysz W, Kamysz E, Silvestri C, Orlando F, Burucca C, Scalise A, Saba V, Scalise G, Giacometti A, Offidani A. Temporin A is effective in MRSA-infected wounds through bactericidal activity and acceleration of wound repair in a murine model. Peptides. 2008;29:520–28.
15. Squarize CH, Castilho RM, Bugge TH, Gutkind JS. Accelerated wound healing by mTOR activation in genetically defined mouse models. Plos One. 2010;5(5):e10643.
16. Castilho RM, Squarize CH, Leelahavanichkul K, Zheng Y, Bugge T, Gutkind JS. Rac1 is required for epithelial stem cell function during dermal and oral mucosal wound healing but not for tissue homeostasis in mice. Plos One. 2010;5(5):e10503.
17. Bibinov N, Knake N, Bahre H, Awakowicz P, Shulz-von der Gathen V. Spectroscopic characterization of an atmospheric pressure -jet plasma source. J Phys D: Appl Phys. 2011;44:345204.
18. Lu Xinpei, Shunqun Wu. On the Active Species Concentrations of Atmospheric Pressure Nonequilibrium Plasma Jets. Plasma Science, IEEE Trans. 2013;41(8):2313–26.